European Journal of Radiology 112 (2019) 112–120

Contents lists available at ScienceDirect

European Journal of Radiology

journal homepage: www.elsevier.com/locate/ejrad

Research article

Whole-tumour histogram analysis of pharmacokinetic parameters from dynamic contrast-enhanced MRI in resectable oesophageal squamous cell carcinoma can predict T-stage and regional lymph node metastasis

Yan-li Chen[a,b,1], Rui Li[a,1], Tian-wu Chen[a,*], Jing Ou[a], Xiao-ming Zhang[a], Fan Chen[a,b], Lan Wu[a], Yu Jiang[a], Maxwell Laws[c], Kamran Shah[c], Bobby Joseph[c], Jiani Hu[c]

[a] Sichuan Key Laboratory of Medical Imaging, and Department of Radiology, Affiliated Hospital of North Sichuan Medical College, 63# Wenhua Road, Nanchong 637000, Sichuan, China
[b] Department of Radiology, Southwest Hospital, Army Medical University (Third Military Medical University), Chongqing, China
[c] Department of Radiology, Wayne State University, Detroit, MI, USA

ARTICLE INFO

Keywords:
Squamous cell carcinoma
Esophagus
Lymphatic metastasis
Magnetic resonance imaging
Perfusion imaging

ABSTRACT

Objective: To identify whether whole-tumour histogram analysis of pharmacokinetic parameters from dynamic contrast-enhanced magnetic resonance imaging (DCE-MRI) could predict T-stage and regional lymph node metastasis (LNM) of resectable oesophageal squamous cell carcinoma (SCC).

Materials and methods: Forty-two consecutive patients with confirmed oesophageal SCC underwent thoracic DCE-MRI. Histogram metrics (median, mean, standard deviation [SD], skewness, kurtosis and entropy) of whole-tumour pharmacokinetic parameters including endothelial transfer constant (K^{trans}), reflux rate (K_{ep}) and fractional extravascular extracellular space volume (V_e) were generated by the Omni-Kinetics software. Histogram datasets were interpreted using the Mann-Whitney U test and receiver operating characteristic (ROC) statistical analyses.

Results: The Mann-Whitney U tests revealed that the median, mean and SD of K^{trans}, the SD and entropy of K_{ep}, and the median, mean and entropy of V_e of T1-2 stage oesophageal SCC were lower when compared with T3 stage (all $Ps < 0.05$); and the ROC analysis showed that the entropy of V_e could reliably distinguish T1-2 stage from T3 stage with an area under ROC (AUC) of 0.773. The Mann-Whitney U tests illustrated that the entropy of K^{trans}, and the median, mean, SD and entropy of K_{ep} were higher while the skewness of K_{ep} was lower in tumours with LNM than without LNM (all $Ps < 0.05$); and the ROC analysis demonstrated that the SD of K_{ep} could best identify tumours with LNM with an AUC of 0.702.

Conclusion: Whole-tumour histogram analysis of pharmacokinetic parameters of oesophageal SCC on DCE-MRI could be used to predict T-stage and regional LNM.

1. Introduction

Oesophageal cancer is the eighth most common malignant tumour and the sixth leading cause of cancer-related death worldwide [1]. The major histological type of this cancer is squamous cell carcinoma (SCC) [2]. Patients with early-stage (T1-2) oesophageal cancer are likely N0, requiring resection alone, while advanced (T3) tumours are likely N + and require neoadjuvant therapy [3]. Therefore, preoperative T staging and prediction of regional lymph node metastasis (LNM) of oesophageal SCC is critical for clinical decision making.

Magnetic resonance imaging (MRI) is increasingly used to investigate the T and N stage of oesophageal SCC [4,5]. Furthermore, Dynamic contrast-enhanced MRI (DCE-MRI) has emerged as a technique to non-invasively evaluate the microcirculation of malignant

Abbreviations: SCC, squamous cell carcinoma; DCE-MRI, dynamic contrast-enhanced magnetic resonance imaging; LNM, lymph node metastasis; SD, standard deviation; ROC, receiver operating characteristic; AUC, area under ROC; EES, extravascular-extracellular space; ROI, region of interest; CT, computed tomography; TR, repetition time; TE, echo time; FOV, field of view; LAVA, liver acquisition with volume acceleration; AIF, arterial input function; ICC, inter-class correlation coefficient

* Corresponding author.
E-mail address: chentw@aliyun.com (T.-w. Chen).
[1] These authors contribute equally to this work.

https://doi.org/10.1016/j.ejrad.2019.01.012
Received 28 September 2018; Received in revised form 6 January 2019; Accepted 13 January 2019

tumours such as breast and rectal cancer [6,7]. DCE-MRI can visually display the enhancement of a target area and semi-quantitatively characterize tumours with time-intensity curves. Also, it can quantitatively evaluate tumours with parameters generated from pharmacokinetic models, illustrated by the dynamic distribution of gadolinium-related contrast agents within the different compartments of a lesion [8–11]. The two-compartment model of DCE-MRI assumes that the contrast agent exchanges between the plasma space and the extravascular-extracellular space (EES), and the forward and backward transfer rate can reflect the permeability of the microvasculature [12].

Recently, DCE-MRI has become a valuable imaging technique for use in the diagnostic workup of oesophageal SCC. Previous studies were limited by the fact they chose only mean values of pharmacokinetic parameters to evaluate the microcirculation of oesophageal SCC [13,14]. However, given the significant intratumour heterogeneity in malignant tumours, a more extensive analysis is needed [15]. Past investigators have established histogram analysis as a means to extract heterogeneity parameters from regions of interest (ROIs) [16]. Whole-tumour analysis, which samples from the entire tumor parenchyma and stroma, may provide a more accurate quantitative assessment of tumour biology. Previously, it has been shown that this technique improves the diagnostic capability of MRI when compared to analyzing a limited sampling region of the tumour [17]. Thus, the aim of our study was to investigate the feasibility of whole-tumour histogram analysis of pharmacokinetic parameters from DCE-MRI for predicting T-stage and regional LNM of oesophageal SCC.

2. Materials and methods

2.1. Patients

The institutional review board of our hospital approved this prospective study, and written informed consent was obtained from each patient.

During the period of February 2016 to December 2017, 50 consecutive patients with biopsy-confirmed oesophageal SCC were enrolled in our study. Inclusion criteria were as follows: (a) the patient did not receive any tumour-related treatment (e.g. radiotherapy and/or chemotherapy) before DCE-MRI examination or surgery; (b) patients had no contraindications for DCE-MRI (e.g. claustrophobia or ferromagnetic metal parts in the patient's body) or surgery (e.g. medically unable to tolerate general anesthesia and/or major thoracic surgery); (c) the tumour with a diameter of less than or equal to 2 cm was considered resectable even if the tumour was staged as T3 and had LNM based on the National Comprehensive Cancer Network (NCCN) guidelines [18]; and (d) the quality of DCE-MRI images was sufficient. The interval between the biopsy and DCE-MRI examination was more than 3 days (mean, 4.56 days; range, 4–7 days), and no bleeding events occurred.

Of the initial patients, no oesophageal SCC involved oesophagogastric junction, 2 patients had received tumour-related treatment prior to DCE-MRI examination and surgery, 4 patients had contraindications for surgery, and 2 patients had poor quality DCE-MRI images on which the pharmacokinetic parameters could not be measured. Ultimately, 42 patients were enrolled into our study. The enrolled patients were scheduled for radical oesophagectomy with three-field lymphadenectomy within two weeks (mean 5.74 days; range 3–11 days) following the DCE-MRI examination. TNM staging was performed according to the postoperative histopathology and American Joint Committee on Cancer (AJCC) criteria [19].

2.2. DCE-MRI technique

DCE-MRI examinations were performed on a 3.0 T superconductive magnet (Discovery MR 750, GE Medical Systems) with a 32-channel surface phased-array body coil in the chest region with respiratory gating and cardiac gating in all enrolled patients. The patient was provided breathing training prior to the imaging session. The patients were examined in the supine position. Axial and sagittal T_2-weighted imaging with fat saturation were obtained for tumour localization, and the scanning parameters were as follows: repetition time (TR) of 3000–4000 ms, echo time (TE) of 85–95 ms, field of view (FOV) of 36 cm × 36 cm, matrix of 352 × 352, and slice thickness of 4 mm. Subsequently, DCE-MRI was performed, which included a pre-contrast T_1 mapping sequence and a dynamic sequence. The pre-contrast T_1 mapping sequence was performed with five consecutive axial three-dimensional (3D) spoiled-gradient recalled-echo sequences for liver acquisition with volume acceleration (LAVA) of multi-flip angles (3°, 6°, 9°, 12° and 15°) in breath-hold mode. Scanning parameters for the T_1 mapping were as follows: TR of 3.3 ms, TE of 1.5 ms, FOV of 36 cm × 36 cm, matrix of 256 × 192, and slice thickness of 6 mm. The dynamic sequence was conducted with the same scanning parameters as pre-contrast T_1 mapping except for a flip angle of 15°, which resulted in a temporal resolution of 7 s. The entire dynamic process lasted for 5 min 4 s with 40 dynamics in free-breathing mode. When the scan for the fourth phase of the dynamic process was started, the contrast agent (0.1 mmol/kg, Omniscan, GE Healthcare) was administered intravenously as a bolus injection at a rate of 2.5 ml per second using a high pressure injector system (Spectris MR Injector System), immediately followed by 20 ml saline flush at the same rate. As described elsewhere [20], baseline images were obtained from the pre-injection dynamic acquisitions and subsequently used to generate time-intensity curves with the DCE-MRI data analysis.

2.3. Data analysis

The DCE-MRI data was transferred to the special post-processing software (Omni-Kinetics; GE Healthcare). Two experienced radiologists (Y.L.C. and T.W.C. with 3 and 20 years of experience in gastrointestinal radiology, respectively) who were blind to the histopathological results, independently performed the data analysis. First, non-rigid registration of the dynamic images was performed by using a framework (a free-form deformation algorithm) to help correct any error of dislocation between consecutive DCE-MRI scans [21]. Second, a pre-contrast T_1 mapping sequence was used to obtain the T_1 value of the tissue before and after contrast agent injection [22]. Third, an arterial input function (AIF) was extracted by manually drawing a circle region of interest (ROI) on the descending aorta. The two-compartment extended-Tofts model was selected to calculate the pharmacokinetic parameters including endothelial transfer constant (K^{trans}, in ml/min), reflux rate (K_{ep}, in ml/min), and fractional extravascular extracellular space volume (V_e, in ml/ml) [23]. Fourth, a series of ROIs covering the whole tumour was continuously manually drawn onto magnified DCE-MRI images (Figs.1–4a). The intraluminal gas and paraesophageal fat were excluded based on the axial T_2-weighted sequence with fat saturation. When performing manual segmentation, the necrosis within the oesophageal SCC was included, this was done to avoid discarding spatially rich information regarding intratumor heterogeneity. Finally, the histogram metrics (mean, median, standard deviation [SD], skewness, kurtosis and entropy) of K^{trans}, K_{ep} and V_e were automatically derived. Skewness describes the degree of asymmetry of the probability distribution: a completely symmetric histogram had a skewness of 0, a histogram with a long right tail had a positive skewness whereas a histogram with a long left tail had a negative skewness. Kurtosis describes the sharpness of the distribution and is a measure of the shape of a histogram: a normal distribution had a kurtosis of 0, a more peaked histogram had a positive kurtosis value. Entropy represents a statistical measure of the 'irregularities' in a histogram. The value of entropy increases with the increase of 'irregularities'. The previous software automatically derived the parametric maps of K^{trans} (Figs. 1–4b), K_{ep} (Figs. 1–4c) and V_e (Figs. 1–4d) of all ROIs within the tumour and the histogram graphs of K^{trans} (Figs. 1–4e), K_{ep} (Figs. 1–4f) and V_e (Figs. 1–4g). The previous data analysis by both experienced

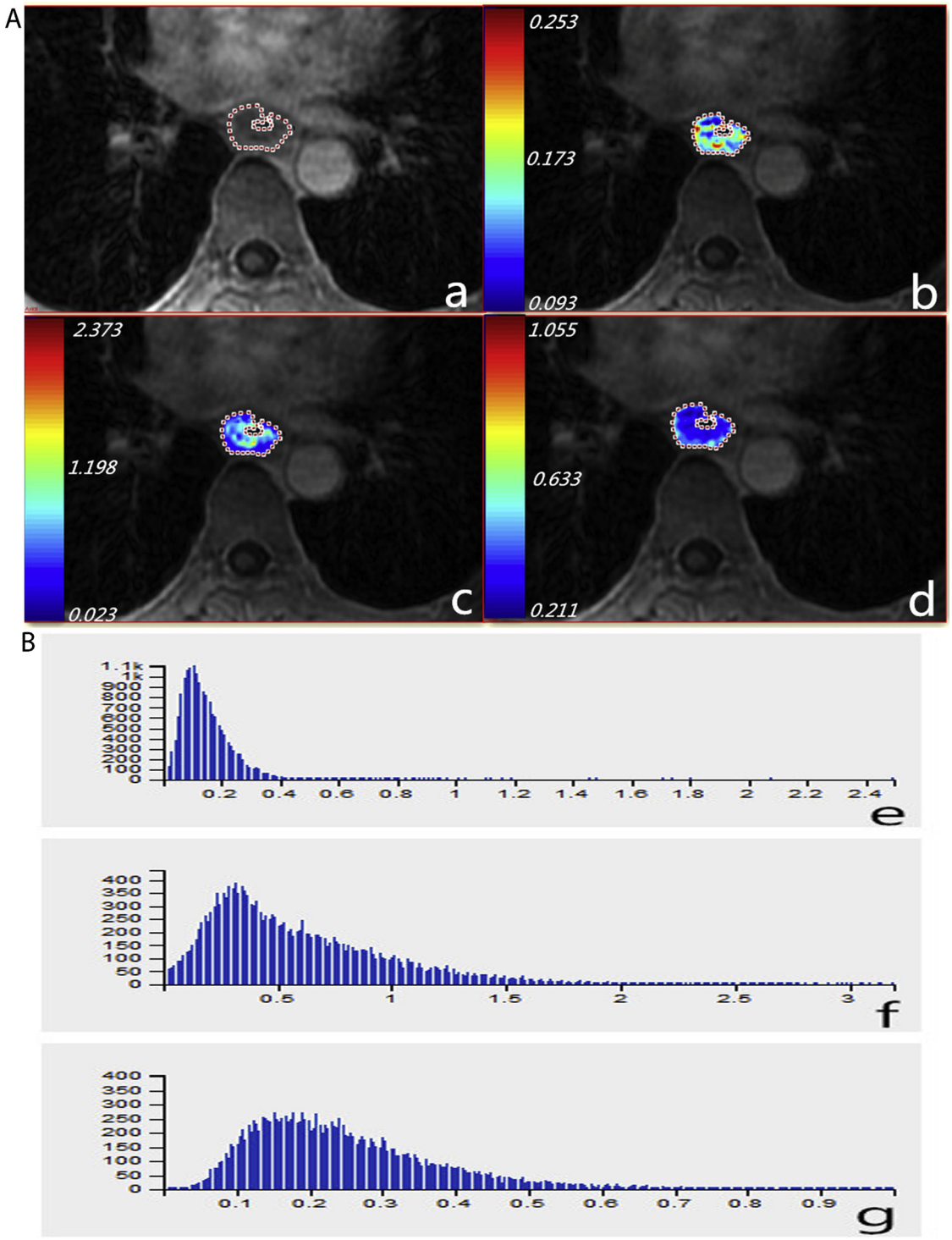

Fig. 1. Image A shows a region of interest (ROI) that has been manually drawn on magnified dynamic contrast-enhanced magnetic resonance image (a) of a 63-year-old male with T3 stage squamous cell carcinoma of the middle thoracic portion of oesophagus without lymph node metastasis. Corresponding colour parametric maps of K^{trans} (b), K_{ep} (c) and V_e (d) are created automatically. The corresponding mean values of K^{trans}, K_{ep} and V_e are 0.129 ml/min, 0.599 ml/min and 0.266 ml/ml, respectively. On Image B, the histogram of K^{trans} (e) demonstrates that the median, mean, standard deviation (SD), skewness, kurtosis and entropy are 0.107 ml/min, 0.129 ml/min, 0.098 ml/min, 4.984, 7.575 and 4.741, respectively; the histogram of K_{ep} (f) shows that the median, mean, SD, skewness, kurtosis and entropy are 0.484 ml/min, 0.599 ml/min, 0.316 ml/min, 1.393, 2.663 and 6.145, respectively; and the histogram of V_e (g) depicts that the median, mean, SD, skewness, kurtosis and entropy are 0.226 ml/ml, 0.266 ml/ml, 0.179 ml/ml, 1.878, 4.692 and 7.012, respectively.

radiologists was used to assess the inter-observer agreement of the histogram metrics of pharmacokinetic parameters measurements. To verify the intra-observer agreement of the histogram metrics measurements, data analysis was repeated by Y.L.C. one month later.

2.4. Statistical analysis

SPSS statistical package (version 13.0 for Windows, SPSS Inc.) was used for statistical analysis. Statistically significant difference was assigned to $Ps < 0.05$.

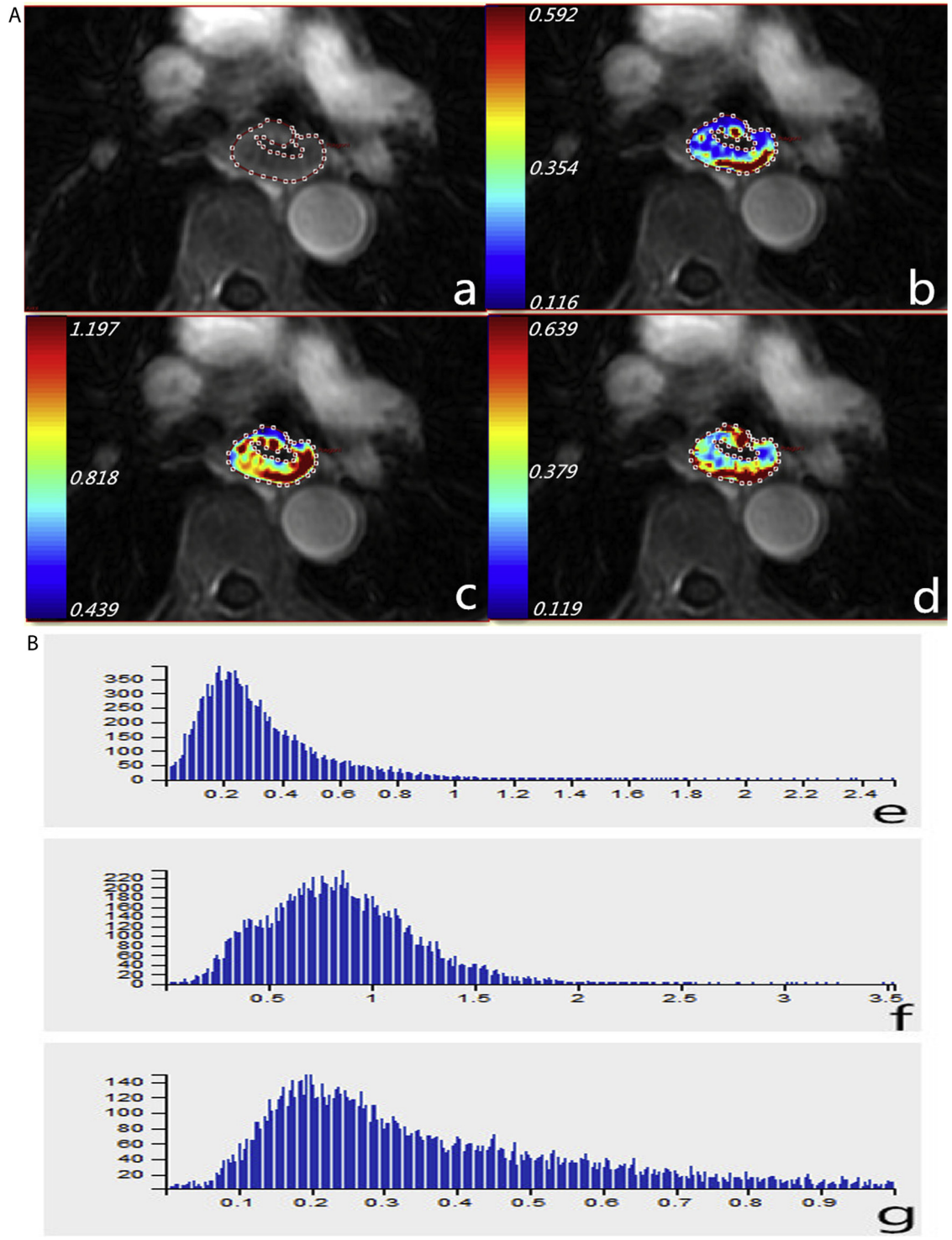

Fig. 2. Image A shows a region of interest (ROI) that has been manually drawn on magnified dynamic contrast-enhanced magnetic resonance image (a) of a 71-year-old male with T3 stage squamous cell carcinoma of the middle thoracic portion of oesophagus with metastasis to one lymph node, and that the colour parametric maps of K^{trans} (b), K_{ep} (c) and V_e (d) are automatically generated. The corresponding mean values of K^{trans}, K_{ep} and V_e are 0.313 ml/min, 0.852 ml/min and 0.388 ml/ml, respectively. On Image B, the histogram of K^{trans} (e) depicts that the median, mean, standard deviation (SD), skewness, kurtosis and entropy are 0.251 ml/min, 0.313 ml/min, 0.238 ml/min, 2.312, 9.018 and 6.116, respectively; the histogram of K_{ep} (f) demonstrates that the median, mean, SD, skewness, kurtosis and entropy are 0.818 ml/min, 0.852 ml/min, 0.379 ml/min, 0.856, 2.030 and 6.697, respectively; and the histogram of V_e (g) shows that the median, mean, SD, skewness, kurtosis and entropy are 0.300 ml/ml, 0.388 ml/ml, 0.260 ml/ml, 1.066, 0.173 and 7.494, respectively.

Inter-observer and intra-observer agreements for the measurements of histogram metrics of pharmacokinetic parameters were evaluated by using the inter-class correlation coefficient (*ICC*) as in the published similar studies [24,25]. The agreement was defined as excellent (*ICC* > 0.90), good (*ICC* = 0.75 - 0.90), moderate (*ICC* = 0.5 - 0.75), and poor (*ICC* < 0.5) [26]. If the inter- and intra-observer agreements were good (*ICC* > 0.75), values of the first measurement by Y.L.C. were regarded as the final values. If not, the mean value of the two

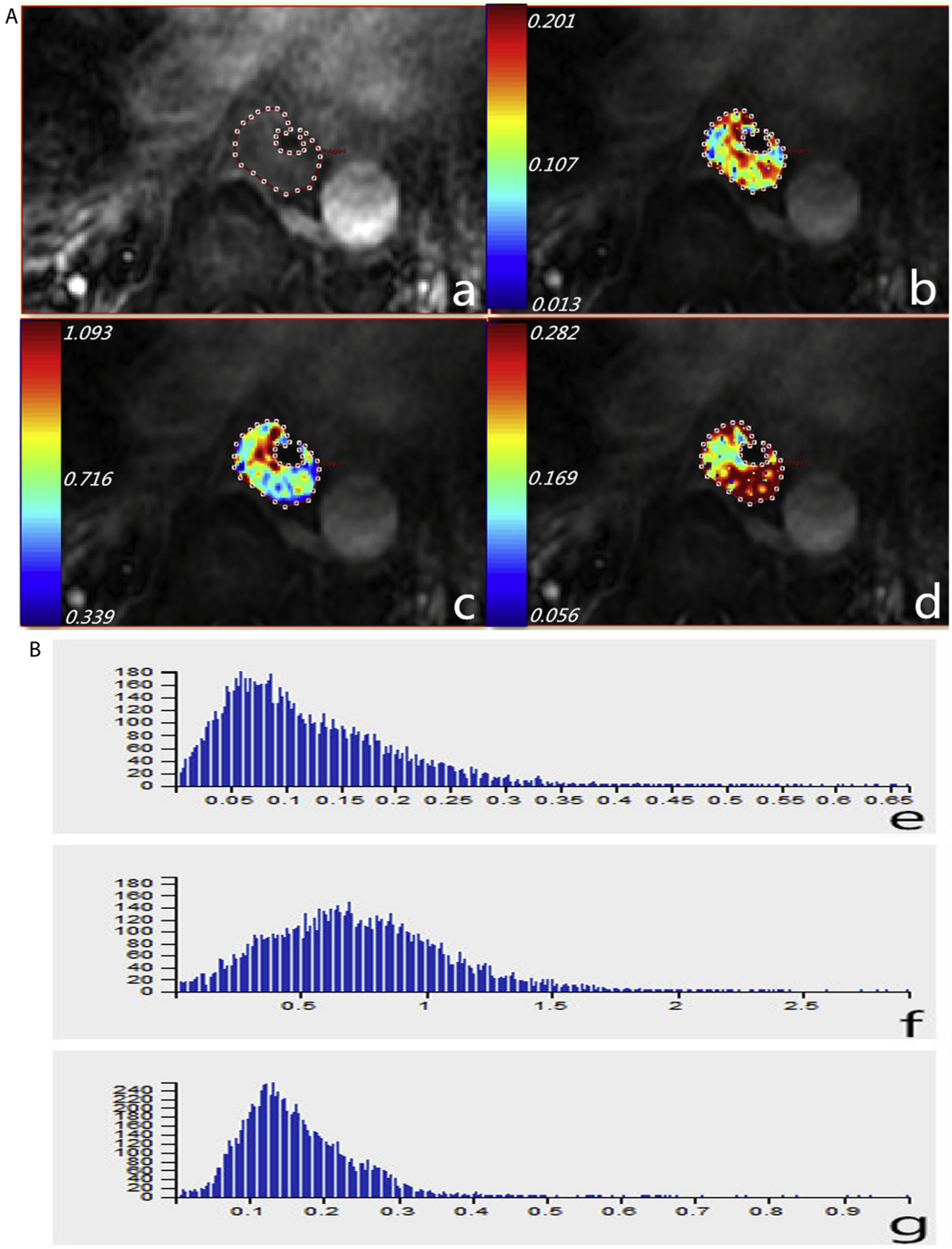

Fig. 3. Image A shows a region of interest (ROI) that has been manually drawn on magnified dynamic contrast-enhanced magnetic resonance image (a) of a 62-year-old male with T2 stage squamous cell carcinoma of the lower thoracic portion of oesophagus with one lymph node involved, and that the colour parametric maps of K^{trans} (b), K_{ep} (c) and V_e (d) are automatically derived. The corresponding mean values of K^{trans}, K_{ep} and V_e are 0.131 ml/min, 0.716 ml/min and 0.190 ml/ml, respectively. On Image B, the histogram of K^{trans} (e) shows that the median, mean, standard deviation (SD), skewness, kurtosis and entropy are 0.107 ml/min, 0.131 ml/min, 0.094 ml/min, 1.689, 4.805 and 6.651, respectively; the histogram of K_{ep} (f) illustrates that the median, mean, SD, skewness, kurtosis and entropy are 0.682 ml/min, 0.716 ml/min, 0.317 ml/min, 0.671, 1.125 and 6.141, respectively; and the histogram of V_e (g) demonstrates that the median, mean, SD, skewness, kurtosis and entropy are 0.169 ml/ml, 0.190 ml/ml, 0.113 ml/ml, 2.729, 15.074 and 6.451, respectively.

measurements by Y.L.C. and the measurement by T.W.C. were to be used in the final analysis.

As the number of tumours in each separate stage was relatively small, for T-stage, we divided the patients into two groups including T1-2 and T3 stages; for N stage, we divided the patients into two groups including N0 and N1-3 stage. The Mann-Whitney U test was performed to compare the histogram metrics between stages T1-2 and T3 and between N0 and N1-3. Bonferroni correction was not used in the Mann-

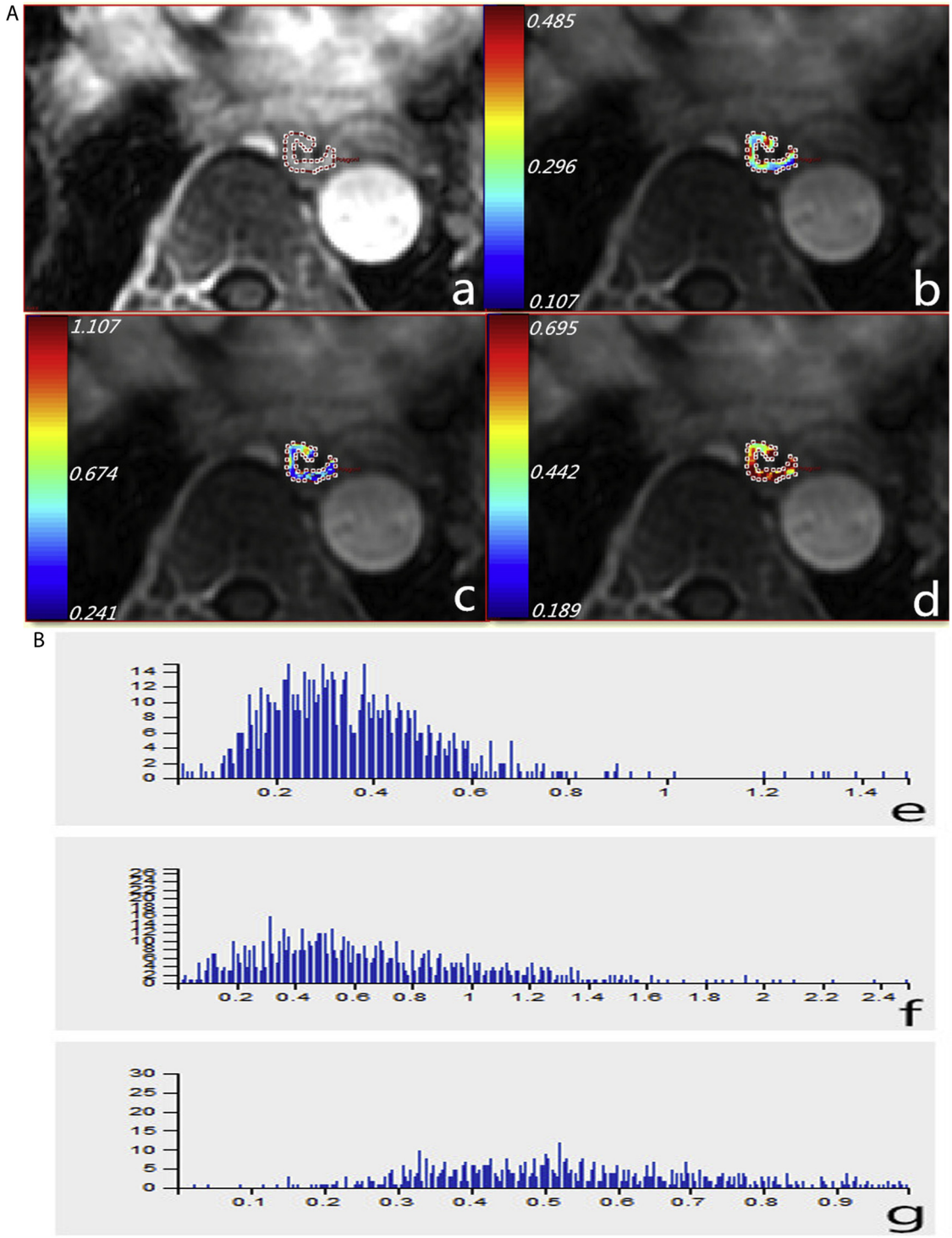

Fig. 4. Image A shows a region of interest (ROI) that has been manually drawn on magnified dynamic contrast-enhanced magnetic resonance image (a) of a 48-year-old male with T1 stage squamous cell carcinoma of the middle thoracic portion of oesophagus with three lymph nodes involved, and that the colour parametric maps of K^{trans} (b), K_{ep} (c) and V_e (d) are automatically generated. The corresponding mean values of K^{trans}, K_{ep} and V_e are 0.328 ml/min, 0.627 ml/min and 0.561 ml/ml, respectively. On Image B, the histogram of K^{trans} (e) shows that the median, mean, standard deviation (SD), skewness, kurtosis and entropy are 0.296 ml/min, 0.328 ml/min, 0.189 ml/min, 1.817, 6.635 and 6.580, respectively; the histogram of K_{ep} (f) depicts that the median, mean, SD, skewness, kurtosis and entropy are 0.552 ml/min, 0.627 ml/min, 0.433 ml/min, 0.977, 1.319 and 6.868, respectively; and the histogram of V_e (g) illustrates that the median, mean, SD, skewness, kurtosis and entropy are 0.529 ml/ml, 0.561 ml/ml, 0.253 ml/ml, 0.068, -0.3644 and 7.222, respectively.

Whitney *U* test, this is in contrast to a similar quantitative study, which used histogram analysis of diffusion-weighted MRI to characterize cervical cancer [27]. Instead, if there was significant difference in the previous test, the receiver operating characteristic (ROC) analysis was performed to test whether and how these indexes could help assess oesophageal SCC of different T-stage and identify oesophageal SCC with regional LNM.

Table 1
Clinical and histopathological characteristics of 42 oesophageal SCC patients.

Age (years)	
Range	42–76
Median	65
Mean ± standard deviation	64.33 ± 7.93
Gender	No. of patients
Male	33
Female	9
Location of the tumour	No. of patients
Upper thoracic oesophagus	2
Middle thoracic oesophagus	29
Lower thoracic oesophagus	11
Differentiation	No. of patients
Well	20
Moderate	21
Poor	1
T stage	No. of patients
T1	6
T2	7
T3	29
N stage	No. of patients
N0	24
N1	9
N2	7
N3	2
Metastatic stage	No. of patients
M0	42
M1	0

Note: The tumours of the lower thoracic oesophagus do not involve the oesophagogastric junction.

3. Results

3.1. Clinical and histopathological characteristics

Table 1 gives an overview about the clinical and histopathological characteristics of our research cohort. All 42 resected lesions were histopathologically proven oesophageal SCC, while the margins of the resected oesophageal segments were found to be uninvolved. In addition, the mean diameter of oesophageal SCC on transverse section was 1.43 cm (ranged from 0.62 cm to 1.96 cm).

3.2. Inter- and intra-observer agreements for the measurements of histogram metrics

Inter- and intra-observer agreements were both good because of the *ICC* > 0.75 (95% confidence interval, 0.837-0.998 and 0.981-0.998, respectively) for the measurements of histogram metrics of pharmacokinetic parameters (Table 2). Therefore, values of the first measurement by Y.L.C. were used for subsequent analysis.

3.3. Histogram metrics for discriminating stage T1-2 from T3

As shown by the Mann-Whitney U tests (Table 3), the median, mean and SD of K^{trans}, the SD and entropy of $K_{ep,}$ and the median, mean and entropy of V_e of T1-2 stage oesophageal SCC were significantly lower when compared with T3 stage (all *Ps* < 0.05). There were no significant differences in the other histogram metrics of whole-tumour pharmacokinetic parameters between T1-2 and T3 stage oesophageal SCC (all *Ps* > 0.05). The previous histogram metrics with significant differences were subsequently used to perform the ROC analysis, and we found that the entropy of V_e was best for discriminating T1-2 from T3 stage oesophageal SCC. The area under the ROC curve (AUC) of the entropy of V_e was 0.773 with an optimal cutoff of 6.48 (Table 4).

3.4. Histogram metrics for identifying tumours with regional LNM

Based on the Mann-Whitney U tests (Table 3), the entropy of K^{trans}, and the median, mean, SD and entropy of K_{ep} were higher whereas the skewness of K_{ep} was lower in tumours with regional lymph node metastasis than without lymph node metastasis (all *Ps* < 0.05). There were no significant differences in the other histogram metrics between oesophageal SCC with and without regional LNM (all *Ps* > 0.05). According to the ROC analysis, the SD of K_{ep} was best for identifying tumours with regional LNM. The AUC of the SD of K_{ep} was 0.702 with an optimal cutoff of 0.32 ml/min (Table 4).

4. Discussion

In this study, we used DCE-MRI to assess the intratumour heterogeneity in oesophageal SCC by whole-tumour histogram analysis, and

Table 2
Inter-class correlation coefficient (ICC) analysis on histogram metrics of pharmacokinetic parameters derived from dynamic contrast-enhanced magnetic resonance imaging.

Kinetic parameters	Histogram metrics	Intra-observer		Inter-observer	
		ICC (95%CI)	*P* value	*ICC* (95%CI)	*P* value
K^{trans}	Median	0.993 (0.987, 0.996)	< 0.001	0.991 (0.984, 0.995)	< 0.001
	Mean	0.992 (0.986, 0.996)	< 0.001	0.990 (0.982, 0.995)	< 0.001
	SD	0.991 (0.983, 0.995)	< 0.001	0.983 (0.968, 0.991)	< 0.001
	Skewness	0.997 (0.995, 0.998)	< 0.001	0.995 (0.991, 0.998)	< 0.001
	Kurtosis	0.996 (0.992, 0.998)	< 0.001	0.994 (0.990, 0.997)	< 0.001
	Entropy	0.996 (0.992, 0.998)	< 0.001	0.990 (0.982, 0.995)	< 0.001
K_{ep}	Median	0.996 (0.993, 0.998)	< 0.001	0.995 (0.991, 0.997)	< 0.001
	Mean	0.995 (0.991, 0.998)	< 0.001	0.994 (0.989, 0.997)	< 0.001
	SD	0.993 (0.987, 0.996)	< 0.001	0.990 (0.982, 0.995)	< 0.001
	Skewness	0.997 (0.994, 0.998)	< 0.001	0.967 (0.940, 0.982)	< 0.001
	Kurtosis	0.995 (0.991, 0.997)	< 0.001	0.912 (0.837, 0.953)	< 0.001
	Entropy	0.994 (0.989, 0.997)	< 0.001	0.985 (0.971, 0.992)	< 0.001
V_e	Median	0.996 (0.993, 0.998)	< 0.001	0.995 (0.991, 0.998)	< 0.001
	Mean	0.997 (0.995, 0.998)	< 0.001	0.996 (0.993, 0.998)	< 0.001
	SD	0.997 (0.994, 0.998)	< 0.001	0.993 (0.988, 0.996)	< 0.001
	Skewness	0.995 (0.990, 0.997)	< 0.001	0.989 (0.980, 0.994)	< 0.001
	Kurtosis	0.990 (0.981, 0.994)	< 0.001	0.979 (0.961, 0.989)	< 0.001
	Entropy	0.995 (0.990, 0.997)	< 0.001	0.985 (0.973, 0.992)	< 0.001

Notes: 95%CI, 95% confidence interval; K^{trans}, endothelial transfer constant; K_{ep}, reflux rate; V_e, fractional extravascular extracellular space volume; and SD, standard deviation.

Table 3
Histogram metrics of whole-tumour pharmacokinetic parameters of oesophageal squamous cell carcinoma between stages T1-2 and T3, and between N0 and N1-3.

Kinetic parameter	Histogram metrics			*P* value
Stage T1-2 vs. T3		**T1-2**	**T3**	
K^{trans}	Median (ml/min)	0.18 ± 0.16	0.26 ± 0.20	0.009
	Mean (ml/min)	0.22 ± 0.18	0.33 ± 0.24	0.011
	SD (ml/min)	0.18 ± 0.15	0.26 ± 0.17	0.008
	Skewness	2.23 ± 1.80	2.70 ± 2.12	0.212
	Kurtosis	13.83 ± 27.43	19.02 ± 28.10	0.114
	Entropy	5.79 ± 1.15	6.14 ± 0.83	0.150
K_{ep}	Median (ml/min)	0.47 ± 0.27	0.54 ± 0.19	0.556
	Mean (ml/min)	0.51 ± 0.26	0.58 ± 0.18	0.458
	SD (ml/min)	0.28 ± 0.12	0.36 ± 0.09	0.002
	Skewness	1.51 ± 1.07	1.03 ± 0.55	0.079
	Kurtosis	3.73 ± 4.21	2.55 ± 3.20	0.276
	Entropy	5.63 ± 1.50	6.65 ± 0.39	0.002
V_e	Median (ml/ml)	0.29 ± 0.22	0.48 ± 0.28	0.001
	Mean (ml/ml)	0.35 ± 0.18	0.47 ± 0.23	0.005
	SD (ml/ml)	0.24 ± 0.10	0.24 ± 0.09	0.754
	Skewness	1.08 ± 1.12	0.55 ± 1.67	0.054
	Kurtosis	4.08 ± 8.13	4.77 ± 11.77	0.354
	Entropy	5.74 ± 1.49	6.98 ± 0.63	< 0.001
Stage N0 vs. N1-3		**N0**	**N1-3**	
K^{trans}	Median (ml/min)	0.21 ± 0.16	0.27 ± 0.22	0.099
	Mean (ml/min)	0.26 ± 0.19	0.34 ± 0.26	0.108
	SD (ml/min)	0.21 ± 0.14	0.27 ± 0.19	0.082
	Skewness	2.84 ± 2.19	2.18 ± 1.73	0.106
	Kurtosis	21.79 ± 33.43	11.58 ± 16.65	0.349
	Entropy	5.81 ± 1.05	6.32 ± 0.72	0.007
K_{ep}	Median (ml/min)	0.47 ± 0.25	0.58 ± 0.15	0.008
	Mean (ml/min)	0.51 ± 0.24	0.62 ± 0.14	0.007
	SD (ml/min)	0.30 ± 0.11	0.38 ± 0.08	< 0.001
	Skewness	1.35 ± 0.91	0.94 ± 0.46	0.032
	Kurtosis	3.54 ± 4.28	2.08 ± 2.05	0.137
	Entropy	6.08 ± 1.23	6.67 ± 0.40	0.029
V_e	Median (ml/ml)	0.40 ± 0.26	0.45 ± 0.30	0.551
	Mean (ml/ml)	0.43 ± 0.21	0.44 ± 0.24	0.937
	SD (ml/ml)	0.25 ± 0.09	0.23 ± 0.10	0.078
	Skewness	0.77 ± 1.47	0.65 ± 1.63	0.771
	Kurtosis	4.12 ± 12.15	5.14 ± 8.60	0.124
	Entropy	6.42 ± 1.36	6.83 ± 0.67	0.551

Notes: Data are means ± standard deviations; K^{trans}, endothelial transfer constant; K_{ep}, reflux rate; V_e, fractional extravascular extracellular space volume; and SD, standard deviation.

identified whether the histogram analysis derived parameters could predict T-stage and regional LNM. We found that whole-tumour histogram analysis of K^{trans}, K_{ep} and V_e obtained from DCE-MRI might predict T-stage and regional LNM of oesophageal SCC. In addition, this study demonstrated that the entropy of V_e may be a useful parameter for distinguishing stages T1-2 from T3, and that the SD of K_{ep} could best identify a tumour with LNM.

Our study showed that the median and mean of K^{trans} of T1-2 stage oesophageal SCC is lower when compared with T3 stage. The potential mechanism might be associated with the histopathological characteristics of malignant lesions. Zhao et al. reported that expression of vascular endothelial growth factor (VEGF) was significantly higher in oesophageal SCC tissues with deep infiltration compared to tissues with only superficial infiltration [28]. VEGF can induce endothelial cell division and migration, enhance microvascular permeability, promote stromal proteolysis, and reduce endothelial cell apoptosis [29]. These microvascular changes allow for a more rapid transfer of the contrast agent from plasma to the EES, ultimately resulting in the higher median and mean of K^{trans} in higher T-staged oesophageal SCC.

Our study demonstrated that the median and mean of V_e is higher in T3 stage than in T1-2 stage. A potential mechanism explaining these results is that the vascular space, which is normally proportional to the EES, may be altered in malignant tumours in order to ensure sufficient nutrients and oxygen supply.

The SD of K^{trans}, the SD and entropy of $K_{ep,}$ and the entropy V_e of T1-2 stage oesophageal SCC could be lower when compared with T3 stage. A possible explanation is that heterogeneity in tumour blood supply increases as tumour grows [30]. Clinically, our study demonstrated that the entropy of V_e could be best for distinguishing T1-2 from T3 stage oesophageal SCC.

As shown in our study, the median and mean of K_{ep} is higher in oesophageal SCC with regional LNM than without lymph node involvement. These findings could be explained by the elevated expression of VEGF. The expression of VEGF in oesophageal SCC with LNM is significantly higher than without LNM [28], which could lead to the higher microvascular permeability in a tumour with LNM. Additionally, our study showed that the skewness of K_{ep} could be lower in oesophageal SCC with regional LNM, suggesting that the distribution of the K_{ep} values could be statistically more positive-skewed in oesophageal SCC without LNM, and that oesophageal SCC without LNM could have lower K_{ep} value than with LNM.

We found that the entropy of K^{trans} and the SD and entropy of K_{ep} is higher in oesophageal SCC with regional LNM than without this metastasis. Recent studies on whole-exome sequencing of multiple tumour samples from patients with pancreatic cancer and renal cell carcinoma have suggested that metastatic clones may develop late in the course of tumour progression [31,32]. As reported by others, the heterogeneity in tumour blood supply tends to increase as tumours grow [30]. As tumour progresses, the development of metastatic clones and the increased heterogeneity could result in the higher entropy of K^{trans}, and the higher SD and entropy of K_{ep} in oesophageal SCC with LNM, which suggests that oesophageal SCC with LNM has more heterogeneous K^{trans} and K_{ep} than without LNM. Clinically, our study demonstrated that the SD of K_{ep} was better than any other histogram metrics for identifying oesophageal SCC with regional LNM.

Our study has several limitations. First, only patients with oesophageal SCC were included in our study. The role of DCE-MRI in the diagnostic work-up of oesophageal adenocarcinoma will be investigated in a later study. Second, as a malignant tumour, oesophageal SCC has poor margins, as differentiation of the tumour from the adjacent normal oesophagus is not uniform, and this variation may result in low reproducibility. However, the dataset from the whole-tumour was large enough that the inclusion of some erroneous data points were not thought to cause severe bias in our study. Third, we only analyzed a portion of histogram metrics in our study to investigate the tumour heterogeneity, but other histogram metrics including percentiles, mode, maximum and minimum were not taken into consideration. The histogram metrics used in our study including the descriptive parameters and distribution parameters such as skewness, kurtosis and entropy can adequately analyze the average value and heterogeneity of microcirculation within oesophageal SCC to a certain degree. Fourth, the patients with T3N+ oesophageal SCC required neoadjuvant therapy before surgery according to the latest version of NCCN guidelines. However, because our study was initiated in February 2016, we performed this study according to NCCN guidelines 2015 version 1. We will carry out our future studies based on the latest version of NCCN guidelines and confirm our results.

5. Conclusions

The whole-tumour cumulative histogram analysis of pharmacokinetic parameters derived from DCE-MRI may be useful in the T-stage and the identification of oesophageal SCC with regional LNM. Clinically, the entropy of V_e could help discriminate T1-2 from T3 stage oesophageal SCC. The SD of K_{ep} could help identify oesophageal SCC

Table 4
Receiver operating characteristic analysis of histogram metrics of whole-tumour pharmacokinetic parameters of oesophageal squamous cell carcinoma for discriminating stages T1-2 from T3, and N0 from N1-3.

Kinetic parameter	Histogram Metrics	Cutoff	Sensitivity (%)	Specificity (%)	AUC
Stages T1-2 vs. T3					
K^{trans}	Median (ml/min)	0.12	69.0	61.5	0.647
	Mean (ml/min)	0.09	89.7	35.9	0.642
	SD (ml/min)	0.10	82.8	46.2	0.648
K_{ep}	SD (ml/min)	0.29	79.3	56.4	0.677
	Entropy	6.07	93.1	46.2	0.672
V_e	Median (ml/ml)	0.25	73.6	59.0	0.693
	Mean (ml/ml)	0.30	73.6	56.4	0.656
	Entropy	6.48	86.2	61.5	0.773
Stages N0 vs. N1-3					
K^{trans}	Entropy	5.85	77.8	54.2	0.640
K_{ep}	Median (ml/min)	0.41	88.9	41.7	0.638
	Mean (ml/min)	0.43	94.4	37.5	0.640
	SD (ml/min)	0.32	77.8	59.7	0.702
	Skewness	1.77	23.6	100	0.612
	Entropy	6.18	94.4	31.9	0.614

Notes: K^{trans}, endothelial transfer constant; K_{ep}, reflux rate; V_e, fractional extravascular extracellular space volume; and SD, standard deviation.

with regional LNM. We hope that our findings will be helpful for distinguishing T1-2 from T3 stage oesophageal SCC, and identifying the status of regional LNM for treatment decision making.

Conflict of interest

There were no conflicts of interest to declare in this study.

Acknowledgements

This work was supported by the National Natural Science Foundation of China (grant no. 81571645), the Sichuan Province Special Project for Youth Team of Science and Technology Innovation (grant no. 2015TD0029), and the Construction Plan for Scientific Research Team of Sichuan Provincial Colleges and Universities (grant no. 15TD0023) for the conduct of the research. The authors thank Dr. Xin Li from GE Healthcare for providing us with the Omni-Kinetics software and teaching us how to perform data analysis with this software.

References

[1] J. Ferlay, I. Soerjomataram, R. Dikshit, et al., Cancer incidence and mortality worldwide: sources, methods and major patterns in GLOBOCAN 2012, Int. J. Cancer 136 (2015) E359–386.
[2] L.A. Torre, F. Bray, R.L. Siegel, J. Ferlay, J. Lortet-Tieulent, A. Jemal, Global cancer statistics, 2012, CA Cancer J. Clin. 65 (2015) 87–108.
[3] T.W. Rice, H. Ishwaran, W.L. Hofstetter, et al., Esophageal cancer: associations with (pN+) lymph node metastases, Ann. Surg. 265 (2017) 122–129.
[4] J. Qu, H. Zhang, Z. Wang, et al., Comparison between free-breathing radial VIBE on 3-T MRI and endoscopic ultrasound for preoperative T staging of resectable oesophageal cancer, with histopathological correlation, Eur. Radiol. 28 (2018) 780–787.
[5] F. Giganti, A. Ambrosi, M.C. Petrone, et al., Prospective comparison of MR with diffusion-weighted imaging, endoscopic ultrasound, MDCT and positron emission tomography-CT in the pre-operative staging of oesophageal cancer: results from a pilot study, Br. J. Radiol. 89 (2016) 20160087.
[6] D.M. Renz, F. Diekmann, F.F. Schmitzberger, et al., Pharmacokinetic approach for dynamic breast MRI to indicate signal intensity time curves of benign and malignant lesions by using the tumor flow residence time, Invest. Radiol. 48 (2013) 69–78.
[7] R.A.P. Dijkhoff, R.G.H. Beets-Tan, D.M.J. Lambregts, G.L. Beets, M. Maas, Value of DCE-MRI for staging and response evaluation in rectal cancer: a systematic review, Eur. J. Radiol. 95 (2017) 155–168.
[8] R.H. Khouli El, K.J. Macura, M.A. Jacobs, et al., Dynamic contrast-enhanced MRI of the breast: quantitative method for kinetic curve type assessment, AJR Am. J. Roentgenol. 193 (2009) W295–300.
[9] M.R. Engelbrecht, H.J. Huisman, R.J. Laheij, et al., Discrimination of prostate cancer from normal peripheral zone and central gland tissue by using dynamic contrast-enhanced MR imaging, Radiology 229 (2003) 248–254.
[10] A. Jackson, J.P. O'Connor, G.J. Parker, G.C. Jayson, Imaging tumor vascular heterogeneity and angiogenesis using dynamic contrast-enhanced magnetic resonance imaging, Clin. Cancer Res. 13 (2007) 3449–3459.
[11] M. Oostendorp, M.J. Post, W.H. Backes, Vessel growth and function: depiction with contrast-enhanced MR imaging, Radiology 251 (2009) 317–335.
[12] T.E. Yankeelov, J.C. Gore, Dynamic contrast enhanced magnetic resonance imaging in oncology: theory, data acquisition, analysis, and examples, Curr. Med. Imaging Rev. 3 (2009) 91–107.
[13] K. Oberholzer, A. Pohlmann, W. Schreiber, et al., Assessment of tumor microcirculation with dynamic contrast-enhanced MRI in patients with esophageal cancer: initial experience, J. Magn. Reson. Imaging 27 (2008) 1296–1301.
[14] J. Lei, Y. Tian, S.C. Zhu, et al., Preliminary study of IVIM-DWI and DCE-MRI in early diagnosis of esophageal cancer, Eur. Rev. Med. Pharmacol. Sci. 19 (2015) 3345–3350.
[15] C.E. Meacham, S.J. Morrison, Tumour heterogeneity and cancer cell plasticity, Nature 501 (2013) 328–337.
[16] N. Just, Improving tumour heterogeneity MRI assessment with histograms, Br. J. Cancer 111 (2014) 2205–2213.
[17] F. Davnall, C.S. Yip, G. Ljungqvist, et al., Assessment of tumor heterogeneity: an emerging imaging tool for clinical practice? Insights Imaging 3 (2012) 573–589.
[18] J.A. Ajani, T.A. D'Amico, K. Almhanna, et al., Esophageal and esophagogastric junction cancers, version 1, J. Compr. Canc. Netw. 13 (2015) 194–227.
[19] T.W. Rice, D.T. Patil, E.H. Blackstone, AJCC/UICC staging of cancers of the esophagus and esophagogastric junction: application to clinical practice, 8th edition, Ann. Cardiothorac. Surg. 6 (2017) 119–130.
[20] E.Y. Chang, X. Li, M. Jerosch-Herold, et al., The evaluation of esophageal adenocarcinoma using dynamic contrast-enhanced magnetic resonance imaging, J. Gastrointest. Surg. 12 (2008) 166–175.
[21] D. Rueckert, L.I. Sonoda, C. Hayes, D.L. Hill, M.O. Leach, D.J. Hawkes, Nonrigid registration using free-form deformations: application to breast MR images, IEEE, Trans. Med. Imaging 18 (1999) 712–721.
[22] F. Khalifa, A. Soliman, A. El-Baz, et al., Models and methods for analyzing DCE-MRI: a review, Med. Phys. 41 (2014) 124301.
[23] P.S. Tofts, G. Brix, D.L. Buckley, et al., Estimating kinetic parameters from dynamic contrast-enhanced T(1)-weighted MRI of a diffusable tracer: standardized quantities and symbols, J. Magn. Reson. Imaging 10 (1999) 223–232.
[24] G. Kuchcinski, E. Le Rhun, A.B. Cortot, et al., Dynamic contrast-enhanced MR imaging pharmacokinetic parameters as predictors of treatment response of brain metastases in patients with lung cancer, Eur. Radiol. 27 (2017) 3733–3743.
[25] H. Hu, X.Q. Xu, H. Liu, X.N. Hong, H.B. Shi, F.Y. Wu, Orbital benign and malignant lymphoproliferative disorders: differentiation using semi-quantitative and quantitative analysis of dynamic contrast-enhanced magnetic resonance imaging, Eur. J. Radiol. 88 (2017) 88–94.
[26] T.K. Koo, M.Y. Li, A guideline of selecting and reporting intraclass correlation coefficients for reliability research, J. Chiropr. Med. 15 (2016) 155–163.
[27] K. Downey, S.F. Riches, V.A. Morgan, et al., Relationship between imaging biomarkers of stage I cervical cancer and poor-prognosis histologic features: quantitative histogram analysis of diffusion-weighted MR images, AJR Am, J. Roentgenol. 200 (2013) 314–320.
[28] Z.H. Zhao, Y. Tian, J.P. Yang, J. Zhou, K.S. Chen, RhoC, vascular endothelial growth factor and microvascular density in esophageal squamous cell carcinoma, World J. Gastroenterol. 21 (2015) 905–912.
[29] H.F. Dvorak, Vascular permeability factor/vascular endothelial growth factor: a critical cytokine in tumor angiogenesis and a potential target for diagnosis and therapy, J. Clin. Oncol. 20 (2002) 4368–4380.
[30] K.G. Brurberg, J.V. Gaustad, C.S. Mollatt, E.K. Rofstad, Temporal heterogeneity in blood supply in human tumor xenografts, Neoplasia 10 (2008) 727–735.
[31] M. Gerlinger, A.J. Rowan, S. Horswell, et al., Intratumor heterogeneity and branched evolution revealed by multiregion sequencing, N. Engl. J. Med. 366 (2012) 883–892.
[32] S. Yachida, S. Jones, I. Bozic, et al., Distant metastasis occurs late during the genetic evolution of pancreatic cancer, Nature 467 (2010) 1114–1117.